

Optimal measurements for quantum spatial superresolution

J. Řeháček,¹ Z. Hradil,¹ D. Koutný,¹ J. Grover,² A. Krzic,² and L. L. Sánchez-Soto^{3,4}

¹*Department of Optics, Palacký University, 17. listopadu 12, 771 46 Olomouc, Czech Republic*

²*ESA—Advanced Concepts Team, European Space Research Technology Centre (ESTEC), Keplerlaan 1, Postbus 299, NL-2200AG Noordwijk, Netherlands*

³*Departamento de Óptica, Facultad de Física, Universidad Complutense, 28040 Madrid, Spain*

⁴*Max-Planck-Institut für die Physik des Lichts, Staudtstraße 2, 91058 Erlangen, Germany*



(Received 22 December 2017; published 3 July 2018)

We construct optimal measurements, achieving the ultimate precision predicted by quantum theory, for the simultaneous estimation of centroid, separation, and relative intensities of two incoherent point sources using a linear optical system. We discuss the physical feasibility of the scheme, which could pave the way for future practical implementations of quantum-inspired imaging.

DOI: [10.1103/PhysRevA.98.012103](https://doi.org/10.1103/PhysRevA.98.012103)

I. INTRODUCTION

Metrology is the science of devising schemes that extract as precise as possible an estimate of the parameters associated with a system. The quantum foundations of this field were laid years ago [1,2]; since then, most of the efforts have been devoted to single-parameter estimation, with a special emphasis in the prominent example of phase [3,4]. The quantum Cramér-Rao lower bound (qCRLB) then provides a saturable bound on the estimation uncertainty, and recipes for finding the optimal measurement attaining that limit are known [5].

The case of multiparameter estimation is considerably more involved [6–8]. Although the equivalent qCRLB was formulated long time ago [9], this bound is not always saturable. The intuitive reason for this is the incompatibility of the measurements for different parameters. The conditions under which the qCRLB can be saturated have been determined [10,11]. The associated optimal measurements have been worked out for pure states [12], but for mixed states the results are fragmentary [13–15].

In this work we will address these problems in the context of the two-point resolution limit for an optical system. In classical optics several criteria exist [16–18] to quantitatively determine these limits, the most famous of which is due to Rayleigh [19].

Most of these criteria exploit properties of the point spread function (PSF) that specifies the intensity response to a point light source. This provides an intuitive picture of the mechanisms limiting resolution, but also has several shortcomings. These mainly stem from the fact that these criteria were developed for the human eye as the main detector. For example, the Rayleigh limit is defined as the distance from the center to the first minimum of the PSF, which can be made arbitrarily small with ordinary linear optics, although at the expense of the side lobes becoming much higher than the central maximum [20]. This confirms that determining the position of the two points becomes also a question of photon statistics rather than being solely described by the Rayleigh limit.

A careful reconsideration of this conundrum has been performed in the framework of quantum estimation

theory [21–28]. This work showed that, in the case of two identical incoherent point sources with *a priori* knowledge of their centroid, the precision of an optimal measurement stays constant at all separations. As a consequence, the Rayleigh limit is subsidiary to the problem and arises because standard direct imaging discards all the phase information contained in the field. These predictions fuelled a number of proof-of-principle experiments [29–32].

While remarkable, this result does not hold in the more general case of two unequally bright sources. In a suitable multiparameter scenario [33], where simultaneous estimation of centroid, separation, and relative brightness was considered, it was found that their estimation precisions decreased with separation [34]. Nonetheless, an appropriate strategy was shown to lead to a significant improvement in precision at small separations over direct imaging for any fixed number of photons. The measurements attaining the ultimate quantum limits for this case are relevant to a number of applications, for example, observational astronomy and microscopy.

II. MODEL AND ASSOCIATED MULTIPARAMETER QUANTUM CRAMÉR-RAO BOUND

To be as self-contained as possible, we first set the stage for our analysis. We assume a linear spatially invariant system illuminated with quasimonochromatic paraxial waves with one specified polarization. We consider one spatial dimension, x denoting the image-plane coordinate.

We phrase what follows in a quantum language that will simplify the following calculations. To a field of complex amplitude $U(x)$ we assign a ket $|U\rangle$, such that $U(x) = \langle x|U\rangle$, $|x\rangle$ being a pointlike source at x . The system PSF is denoted by $I(x) = |\langle x|\Psi\rangle|^2 = |\Psi(x)|^2$, so that $\Psi(x)$ can be interpreted as the amplitude PSF.

Two point sources, of different intensities and separated by a distance s , are imaged by that system. Since they are incoherent with respect to each other, the total signal must be depicted as a density operator,

$$\varrho_\theta = q\varrho_+ + (1-q)\varrho_-, \quad (1)$$

where q and $1 - q$ are the intensities of the sources (the total intensity is normalized to unity). The individual components $\varrho_{\pm} = |\Psi_{\pm}\rangle\langle\Psi_{\pm}|$ are just x -displaced PSF states; that is, $\langle x|\Psi_{\pm}\rangle = \langle x - s_0 \mp s/2|\Psi\rangle$, so that they are symmetrically located around the geometric centroid s_0 . Note that

$$|\Psi_{\pm}\rangle = \exp[-i(s_0 \pm s/2)P]|\Psi\rangle, \quad (2)$$

where P is the momentum operator, which generates displacements in the x variable, and acts as a derivative $P \mapsto -i\partial_x$.

The measured density matrix depends on the centroid s_0 , the separation s , and the relative intensities of the sources q . This is indicated by the vector $\theta = (s_0, s, q)^t$. Our task is to estimate the values of θ through the measurement of some observables on ϱ_{θ} .

In this multiparameter estimation scenario, the central quantity is the quantum Fisher information matrix (qFIM) [35]. This is a natural generalization of the classical Fisher information, which is a mathematical measure of the sensitivity of a quantity to changes in its underlying parameters. However, the qFIM is optimized over all the possible measurements. It is defined as

$$Q_{\alpha\beta}(\theta) = \frac{1}{2}\text{Tr}(\varrho_{\theta}\{L_{\alpha}, L_{\beta}\}), \quad (3)$$

where the Greek indices run over the components of the vector θ and $\{\cdot, \cdot\}$ denotes the anticommutator. Here, L_{α} stands for the symmetric logarithmic derivative (SLD) [9] with respect the parameter θ_{α} :

$$\frac{1}{2}(L_{\alpha}\varrho_{\theta} + \varrho_{\theta}L_{\alpha}) = \partial_{\alpha}\varrho_{\theta}, \quad (4)$$

with $\partial_{\alpha} = \partial/\partial\theta_{\alpha}$.

The qFIM is a distinguishability metric on the space of quantum states and leads to the multiparameter qCRLB [5,8] for a single detection event:

$$\text{Cov}(\hat{\theta}) \geq Q^{-1}(\theta), \quad (5)$$

where $\text{Cov}(\hat{\theta})$ is the covariance matrix for a locally unbiased estimator $\hat{\theta}$ of the quantity θ . Its matrix elements are $\text{Cov}_{\alpha\beta}(\hat{\theta}) = \mathbb{E}[(\hat{\theta}_{\alpha} - \theta_{\alpha})(\hat{\theta}_{\beta} - \theta_{\beta})]$, $\mathbb{E}[Y]$ being the expectation value of the random variable Y . The above inequality should be understood as a matrix inequality. In general, we can write $\text{Tr}[\mathcal{C}\text{Cov}(\hat{\theta})] \geq \text{Tr}[\mathcal{C}Q^{-1}(\theta)]$, where \mathcal{C} is some positive cost matrix, which allows us to asymmetrically prioritise the uncertainty cost of different parameters.

Unlike for a single parameter, the collective bound in Eq. (5) is not always saturable, as the measurements for different parameters may be incompatible [2]. The multiparameter qCRLB can be saturated provided

$$\text{Tr}(\varrho_{\theta}[L_{\alpha}, L_{\beta}]) = 0, \quad (6)$$

where $[\cdot, \cdot]$ is the commutator. This condition is necessary and sufficient for pure states [10,11], upon which the criterion is equivalent to the existence of some pair of SLDs that commute. It is then possible to find an optimal measurement as the common eigenbasis of these SLDs. For mixed states, this criterion has been discussed by a number of authors [36] and has met some small inconsistencies in its usage, being variously identified as sufficient [37] or necessary and sufficient [38]. Reference [39] offers a clear account of this question. For our particular case, Eq. (6) is fulfilled whenever the PSF amplitude

is real [34], $\Psi(x)^* = \Psi(x)$, which will be assumed henceforth ensuring that the parameters are therefore compatible.

For the model we are considering, and after a lengthy calculation [34], we obtain a compact expression for the qFIM; viz

$$Q = 4 \begin{pmatrix} p^2 + 4q(1-q)\wp^2 & (q-1/2)p^2 & -iw\wp \\ (q-1/2)p^2 & p^2/4 & 0 \\ -iw\wp & 0 & \frac{1-w^2}{4q(1-q)} \end{pmatrix}, \quad (7)$$

which depends solely on the quantities

$$\begin{aligned} w &\equiv \langle\Psi_{\pm}|\Psi_{\mp}\rangle = \langle\Psi|\exp(i\wp P)|\Psi\rangle, \\ p^2 &\equiv \langle\Psi_{\pm}|P^2|\Psi_{\pm}\rangle = \langle\Psi|P^2|\Psi\rangle, \\ \wp &\equiv \pm\langle\Psi_{\pm}|P|\Psi_{\mp}\rangle = \langle\Psi|\exp(i\wp P)P|\Psi\rangle. \end{aligned} \quad (8)$$

The quantity p^2 is determined by the shape of the PSF, whereas both w and \wp (which is purely imaginary) depend on the separation s .

Only for equally bright sources, $q = 1/2$, the measurement of s is uncorrelated with the other parameters. In general, when $q \neq 1/2$ the separation is correlated with the centroid (via the intensity term $q - 1/2$) and the centroid is correlated with the intensity (via p^2).

The individual parameter θ_{α} can be estimated with a variance satisfying $\text{Var}(\hat{\theta}_{\alpha}) \geq (Q^{-1})_{\alpha\alpha}(\theta)$. It is convenient to use the inverses of the variances $H_{\alpha} = 1/\text{Var}(\theta_{\alpha})$, usually called the precisions [40]. By inverting the QFIM and taking the limit $s \rightarrow 0$, they turn out to be [34]

$$\begin{aligned} H_{s_0}^Q &\simeq \mathcal{Q}^2 G_{22} s^2 + O(s^4), \\ H_s^Q &\simeq \frac{\mathcal{Q}^2}{4(1-\mathcal{Q}^2)} G_{22} s^2 + O(s^4), \\ H_q^Q &\simeq \frac{1}{\mathcal{Q}^2} G_{22} s^4 + O(s^6), \end{aligned} \quad (9)$$

where

$$\begin{aligned} \mathcal{Q}^2 &= 4q(1-q) < 1, \\ G_{22}^Q &= \text{Var}(P^2) = \langle\Psi|P^4|\Psi\rangle - \langle\Psi|P^2|\Psi\rangle^2. \end{aligned} \quad (10)$$

The superscript Q indicates that the quantities are evaluated from the quantum matrix Q .

III. OPTIMAL MEASUREMENTS

We shall focus on finding measurements attaining the quantum limit, thus offering significant advantages with respect to conventional direct intensity measurements. In the general case of unequally bright sources ($q \neq 1/2$), the lack of symmetry makes this issue challenging and one cannot expect to find closed-form expressions for the optimal positive operator valued measures (POVMs) for all the values of the source parameters. However, this becomes viable when separations get very small. As already discussed, this is the most interesting regime, where conventional imaging techniques fail.

We start by specifying a basis in the signal space. A suitable choice is the set $\{|\Psi_n\rangle\}$ defined in terms of the spatial

derivatives of the amplitude PSF:

$$\langle x|\Psi_n\rangle = \frac{\partial^n}{\partial x^n}\Psi(x-x_0), \quad n=0,1,2,\dots, \quad (11)$$

where x_0 is an arbitrary displacement in the x representation. We convert this set into an orthonormal basis $\{|\Phi_n\rangle\}$ by the standard Gram-Schmidt process. In this basis, all results can be expressed in a PSF-independent form. Moreover, signals well centered on the origin and with small separation, are represented by low-dimensional states; i.e., $\varrho_\theta \rightarrow |\Phi_0\rangle\langle\Phi_0|$ for $s_0 \rightarrow x_0$, and $s \rightarrow 0$.

To estimate three independent parameters, the required POVM must have at least four elements. We therefore consider the following class of measurements $\Pi_j = |\pi_j\rangle\langle\pi_j|$, $j=0, \dots, 2$ and $\Pi_3 = \mathbb{1} - \Pi_0 - \Pi_1 - \Pi_2$, so only three of these are independent. The first three POVM elements are defined in a four-dimensional subspace, with basis $\{|\Phi_0\rangle, \dots, |\Phi_3\rangle\}$, wherein we expand $|\pi_j\rangle$ ($j=0, \dots, 2$) as

$$|\pi_j\rangle = \sum_{k=0}^3 C_{jk}|\Phi_k\rangle. \quad (12)$$

Obviously, the projectors $|\pi_j\rangle\langle\pi_j|$ must be linearly independent. In addition, we impose the following set of conditions

$$\begin{array}{ccc} & |\Phi_0\rangle & |\Phi_1\rangle, \\ |\pi_0\rangle & C_{00} = 0 & C_{01} \neq 0, \\ |\pi_1\rangle & C_{10} = 0 & C_{11} \neq 0, \\ |\pi_2\rangle & C_{20} \neq 0 & C_{21} \neq 0, \end{array} \quad (13)$$

where the row index can be permuted. In this way, two of the three rank-one projectors are orthogonal to the signal PSF Φ_0 , a crucial factor boosting the performance of the measurement. We stress that, by changing the displacement x_0 , the basis and the measurement itself is displaced.

Next, we expand the signal components in the small parameter. We define $a_\pm = s_0 \pm s - x_0$, so we have $\langle x|\Psi_\pm\rangle = \Psi(x-x_0-a_\pm)$, and the expansion in a_\pm gives

$$\begin{aligned} \langle x|\Psi_\pm\rangle &= \sum_m \frac{(-a_\pm)^m}{m!} \frac{\partial^m}{\partial x^m}\Psi(x-x_0) = \sum_m \frac{(-a_\pm)^m}{m!} \langle x|\Psi_m\rangle \\ &= \langle x|\sum_n |\Phi_n\rangle \sum_m \frac{(-a_\pm)^m}{m!} G_{nm}, \end{aligned} \quad (14)$$

where $G_{nm} = \langle \Phi_n|\Psi_m\rangle$ [note that G_{22} in Eq. (10) is consistent with this general definition]. Keeping terms up to the fourth power, we get

$$\begin{aligned} |\Psi_\pm\rangle &\simeq \left(G_{00} + \frac{a_\pm^2}{2}G_{02} + \frac{a_\pm^4}{24}G_{04}\right)|\Phi_0\rangle \\ &+ \left(a_\pm G_{11} + \frac{a_\pm^3}{6}G_{13}\right)|\Phi_1\rangle \\ &+ \left(\frac{a_\pm^2}{2}G_{22} + \frac{a_\pm^4}{24}G_{24}\right)|\Phi_2\rangle + \frac{a_\pm^3}{6}G_{33}|\Phi_3\rangle. \end{aligned} \quad (15)$$

Notice that for real amplitude PSFs, all G s carrying both odd and even subscripts are zero. This follows from the fact that $\langle \Psi_n|\Psi_m\rangle = 0$, and hence $\langle \Psi|P^{m+n}|\Psi\rangle = 0$ for any combination of odd and even subscripts, whenever the wavefunction is real. We also have $G_{nm} = 0$ for all $n > m$, by

construction of the basis set, which makes a basis function orthogonal to all lower-order nonorthogonal functions, as the latter span a subspace that the former is orthogonal to.

We are set to evaluate the probabilities,

$$p_j = q\langle\Psi_+|\Pi_j|\Psi_+\rangle + (1-q)\langle\Psi_-|\Pi_j|\Psi_-\rangle, \quad (16)$$

and the corresponding classical Fisher information matrix per detection event,

$$F_{\alpha\beta} = \sum_{j=0}^3 \frac{(\partial_\alpha p_j)(\partial_\beta p_j)}{p_j}. \quad (17)$$

The maximum of the classical Fisher information F is its quantum version Q , as Q is optimized over all POVMs. The corresponding precisions are thus related by $H_\alpha^Q \geq H_\alpha$.

Our initial strategy is to align the center of the measurement Eq. (12) with the signal centroid by letting $x_0 = s_0$. The calculation of the precisions turns out to be a very lengthy task, yet the final result is surprisingly simple:

$$H_\alpha = \lambda H_\alpha^Q. \quad (18)$$

Therefore, H_α differs from the quantum limit precision by a factor

$$\lambda = \mathcal{Q}^2 \mathcal{A}, \quad \mathcal{A} = \frac{(C_{01}C_{12} - C_{02}C_{11})^2}{C_{01}^2 + C_{11}^2} < 1. \quad (19)$$

The coefficient λ consists of the product of two factors: one depending solely on the intensities [as defined in Eq. (10)], the other depending on the measurement. The latter one will be called the quality factor of the measurement. Conditions Eq. (13) are crucial for deriving relations Eqs. (18) and (19): Violating them makes the dominant terms of H_α disappear and kills the superresolution. One pertinent example would be projection on the basis set $|\Phi_k\rangle$: $C_{jk} = \delta_{jk}$ as for example projections on a set of Hermite-Gauss modes for a Gauss PSF advocated in Refs. [21] and [25], among others. Such projections can be optimal for estimating separation, but ultimately fail when separation, centroid, and intensity are to be estimated together in a multiparameter scenario considered here.

Going back to our result, two remarks are in order here. First, the performance of the measurement Eq. (12), when aligned with the centroid, scales with the same power of s as the quantum limit does. The quantum limit is attained, but for a separation independent factor. This is true for all real-valued PSFs, no matter how we set the remaining free parameters of the measurement. Second, by optimizing those free parameters, the separation-independent factor λ can be made arbitrarily close to $\lambda_{\max} = \mathcal{Q}^2$. Hence, for balanced signals ($q = 1/2$), $\lambda_{\max} \rightarrow 1$ and the measurement Eq. (12) becomes optimal. Conversely, for unbalanced signals, the measurement is suboptimal and its performance worsens with q , approaching the limit $\lambda \rightarrow 0$ when $q \rightarrow 0$ and $q \rightarrow 1$.

Next, we show that quantum limits can be saturated for any q by optimizing the displacement x_0 . The key point is that in the limit $s \ll 1$, the precisions $H_\alpha(x_0)$, when considered as a function of the measurement displacement x_0 , take a Lorentzian shape, as can be appreciated in Fig. 1 for the particular case of $H_s(x_0)$. On decreasing the signal separation, the Lorentzian narrows down, with its center approaching the

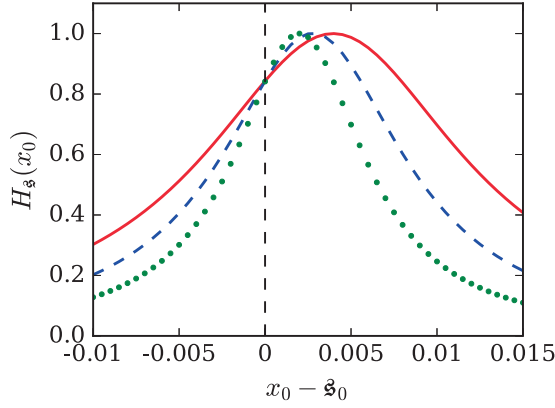


FIG. 1. The precision H_s of the separation for point objects with relative intensities $q = 0.3$ and $s = 0.02$ (red solid line), $s = 0.014$ (blue broken line), and $s = 0.01$ (green dots) as a function of misalignment $x_0 - s_0$ between the measurement displacement and the centroid. The maxima of the Lorentzians are normalized to unity to make the changes in widths and centers apparent.

signal centroid. We therefore adopt the model

$$H_s(x_0) = \frac{\ell_1 s^2}{1 + \frac{\ell_2(x_0 - s_0 + \ell_3 s)^2}{s^2}}. \quad (20)$$

The parameters can be identified by expanding H_s in s and $x_0 - s_0$:

$$\ell_1 s^2 = \mathcal{A} H_s^Q, \quad \ell_2 = \frac{1}{q(1-q)}, \quad \ell_3 = \frac{1}{2}(1-2q). \quad (21)$$

This uncovers the optimal displacement and precisions

$$x_0^{\text{opt}} = \arg \max_{x_0} H_s(x_0) = s_0 - \frac{1}{2}s(1-2q), \quad (22)$$

$$H_s(x_0^{\text{opt}}) = \mathcal{A} H_s^Q.$$

This is the central result of this paper. The optimal choice of displacement is precisely

$$x_0^{\text{opt}} = (1-q)(s_0 - s/2) + q(s_0 + s/2), \quad (23)$$

so that the weighted centroid, rather than the geometrical centroid, is relevant to align the measurement. Note that the weighted centroid only coincides with the center of mass of the PSF when the PSFs are symmetric. By optimizing the measurement displacement x_0 , the intensity dependent \mathcal{Q}^2 term is removed from Eqs. (18) and (19) and the qCRLBs are saturated for all the signal parameters simply by letting $\mathcal{A} \rightarrow 1$. As this can be done in infinitely many ways, we conclude there are infinitely many measurements attaining the quantum limit in multiparameter superresolution imaging. They can be constructed following our recipe for any real-valued amplitude PSF.

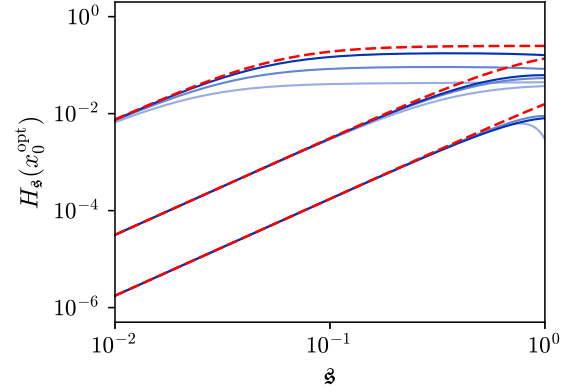


FIG. 2. The precision $H_s(x_0)$ for an optimally displaced measurement Eq. (24) (blue lines) as compared to the quantum limit (9) (red broken lines). The lines are grouped by the intensity difference: $q = 0.49$ (top), $q = 0.35$ (middle), and $q = 0.1$ (bottom). Within each group (light to dark) $\phi = \pi/4, 7\pi/20$, and $9\pi/20$, respectively. Notice the fast convergence towards the quantum limit as $s \rightarrow 0$. A Gaussian PSF of a unit width $\sigma = 1$ is assumed.

IV. EXAMPLES

To illustrate our result with a concrete example, we construct three orthogonal vectors through

$$|\pi_{0,1}\rangle = \begin{pmatrix} 0 \\ \frac{\sin(\phi/2)}{\sqrt{1+\cos\phi}} \\ \pm \frac{\cos(\phi/2)}{\sqrt{1+\cos\phi}} \\ -\sqrt{\frac{\cos\phi}{1+\cos\phi}} \end{pmatrix}, \quad |\pi_2\rangle = \begin{pmatrix} \sqrt{\frac{2\cos\phi}{1+3\cos\phi}} \\ \sqrt{\frac{2\cos\phi}{1+3\cos\phi}} \\ 0 \\ \sqrt{\frac{1-\cos\phi}{1+3\cos\phi}} \end{pmatrix}, \quad (24)$$

with $0 < \phi < \pi/2$ in the $|\Phi_k\rangle$ -representation, to build a family of POVMs according to the recipe Eq. (12). This measurement satisfies all the requirements, and the quality factor becomes $\mathcal{A} = 1$, so that the quantum limit is attained for any real-valued PSF as long as $s \ll \sigma$.

The theory thus far is largely independent of the actual form of the PSF. To be more specific, we adopt a Gaussian PSF, with unit width $\sigma = 1$, which will serve from now on as our basis unit length. The associated orthonormal basis is then a set of displaced Hermite-Gauss modes

$$\Phi_n(x) = \frac{1}{(2\pi)^{\frac{1}{4}} 2^{\frac{n}{2}} \sqrt{n!}} H_n\left[\frac{(x - x_0^{\text{opt}})/\sqrt{2}}{\sqrt{2}}\right] \times \exp\left[-\frac{1}{4}(x - x_0^{\text{opt}})^2\right], \quad (25)$$

where $H_n(x)$ are the Hermite polynomials. In this case, we have then $G_{22} = 1/8$.

Figure 2 shows the resulting precision H_s as a function of s on a log-log scale for different intensities q and different measurements of the family Eq. (24). Direct numerical evaluation of the Fisher information Eq. (17) was done using a computational basis $\{\Phi_n\}$ of dimension 30 and no further approximation. With $s \rightarrow 0$ all precisions quickly converge towards the quantum limit and all the measurements Eq. (24) become optimal. Notice however that performances over a wider range of separations are sensitive to measurement

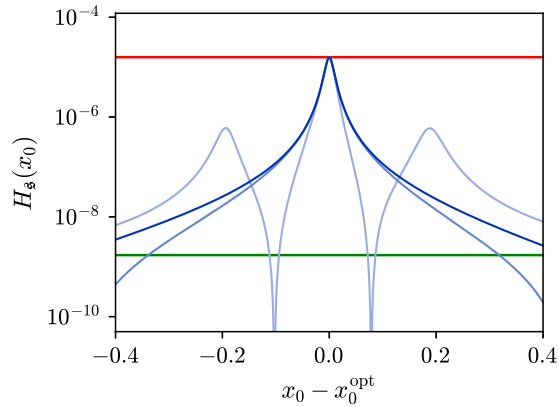


FIG. 3. The precision H_s for misaligned measurements Eq. (24) (solid blue lines) compared to the corresponding quantum (top red) and direct imaging (bottom green) limits. The parameters of the measurements are $\phi = \pi/20$ (light blue), $\pi/2$ (light blue), and $9\pi/20$ (dark blue). Observe the log vertical scale. A Gaussian PSF of a unit width $\sigma = 1$ is assumed; and the sources satisfy $\varsigma = 0.03$ and $\eta = 0.1$.

parameter ϕ and values close to $\phi = \pi/2$ provide the best overall performance.

Having potential applications of our proposed detection scheme in mind we realize that achieving the quantum limits requires knowing the true values of the measured parameters. In particular, the measurement must be optimally displaced to reach the quantum limits and this displacement, through Eq. (22), depends on all the unknown signal parameters. Consequently different displacements should be used for different signals.

Can one hope to saturate the quantum limits for all signals with a fixed measurement? Unfortunately, the answer is negative. Let us consider the estimation of a signal with strongly overlapping components $\varsigma \ll 1$ of highly unequal intensities $\eta \rightarrow 0$ (the same analysis can be carried out for $\eta \rightarrow 1$), so that the weak component is outshined. To gain significant information about the weak component, the bright one must be almost completely suppressed in one of the measurement outputs. This is ensured by projecting the signal on a state that is nearly orthogonal to the bright component. That crucial projection, though, depends on both the signal centroid and separation.

Our optimal measurement also behaves in this way. Let us look at the value of x_0^{opt} in the limit $\eta \rightarrow 0$; i.e., when $|\Psi_-\rangle$ is the bright component. In this case, $x_0^{\text{opt}} \rightarrow \varsigma_0 - \varsigma$ coincides with the center of the bright component. But, this means that $|\Phi_0\rangle = |\Psi_-\rangle$ and the two outputs described by $|\pi_0\rangle$ and $|\pi_1\rangle$ project on subspaces orthogonal to the bright component, as anticipated.

In practice, the performance will be compromised by any misalignment with respect to x_0^{opt} . This effect is examined in Fig. 3, where the quantum limit and the direct intensity imaging are compared with different misaligned measurements Eq. (24). Being about two orders of magnitude below the Rayleigh limit, such imperfections cause a loss of precision. Even then, the advantage with respect to direct imaging persists over a wide range of displacements x_0 , demonstrating the robustness of our detection scheme. Again, setting $\phi \approx \pi/2$ seems to be the best option. For this particular example, the

measurement can be misaligned by as much as 0.4σ from x_0^{opt} and still beat the direct imaging limits in measuring separations two orders of magnitude below the Rayleigh limit.

Such an inherent robustness of optimal detection schemes hints at using adaptive strategies to achieve the quantum limits. One plausible way would be to spend a portion of the photon pool to obtain a first estimate of the optimal displacement $\hat{x}_0^{\text{opt}} = \hat{\varsigma}_0 - \hat{\varsigma}(1 - 2\hat{\eta})/2$. Since this quantity is closely related to the weighted centroid, direct imaging can be used in this step. Then, the estimated \hat{x}_0^{opt} can be used with the optimal measurement Eq. (24) in the next step to refine the estimates of the signal parameters and so forth.

Having considered the fundamental aspects of the problem, how does one implement the optimal measurement in practice for one particular setting of the displacement? This amounts to performing simultaneous projections on three mutually orthogonal states. There exists a unitary transformation taking this triplet into another set of orthogonal vectors, where the latter set is experimentally feasible. For example, the optimal projections can be mapped on three different pixels of a CCD camera. Unitary transformations of this kind can be always realized with a set of nonabsorbing masks. Alternatively, giving up some performance, the implementation can be facilitated by splitting the signal beam and measuring the three projections separately. This leads to a photon loss and a threefold decrease of the precisions H_α , which can be tolerated for sufficiently small separations.

V. CONCLUSIONS

We have examined the ultimate limits for the simultaneous estimation of centroid, separation, and relative intensities of two incoherent point sources. Our results indicate that the optimal sub-Rayleigh resolution limit can be achieved for any real-valued amplitude PSF provided the system output is projected onto a suitable complete set of modes. Particularly useful modes can be generated from the derivatives of the system PSF, which in the limit of small separations can access all available information with a few projections.

For equally bright sources, our proposed projection is optimal whereas, for unbalanced signals, its performance deteriorates with the parameter η . While some of our findings were illustrated explicitly for Gaussian PSFs, our framework is general and can be applied to other relevant cases.

All in all, this constitutes an important application of multiparameter quantum estimation theory to a more realistic imaging setting. Our analysis provides a toolbox for achieving optimal resolution and paves the way for further experimental demonstrations and innovative solutions in scientific, industrial, and biomedical domains.

ACKNOWLEDGMENTS

We acknowledge financial support from the Grant Agency of the Czech Republic (Grant No. 18-04291S), the Palacký University (Grant No. IGA_PrF_2018_003), the European Space Agency's ARIADNA scheme (Contract No. 4000120780/17/NL/LF/as), and the Spanish MINECO (Grant No. FIS2015-67963-P).

- [1] C. W. Helstrom, *Quantum Detection and Estimation Theory* (Academic Press, New York, 1976).
- [2] A. S. Holevo, *Probabilistic and Statistical Aspects of Quantum Theory*, 2nd ed. (North Holland, Amsterdam, 2003).
- [3] V. Giovannetti, S. Lloyd, and L. Maccone, Advances in quantum metrology, *Nat. Photon.* **5**, 222 (2011).
- [4] R. Demkowicz-Dobrzanski, M. Jarzyna, and J. Kolodnyski, Quantum limits in optical interferometry, *Prog. Opt.* **60**, 345 (2015).
- [5] S. L. Braunstein and C. M. Caves, Statistical Distance and the Geometry of Quantum States, *Phys. Rev. Lett.* **72**, 3439 (1994).
- [6] H. Yuen and M. Lax, Multiple parameter quantum estimation and measurement of nonselfadjoint observables, *IEEE Trans. Inf. Theory* **19**, 740 (1973).
- [7] V. P. Belavkin, Generalized uncertainty relations and efficient measurements in quantum systems, *Theor. Math. Phys.* **26**, 213 (1976).
- [8] M. Szczykulska, T. Baumgratz, and A. Datta, Multi-parameter quantum metrology, *Adv. Phys.* **X 1**, 621 (2016).
- [9] C. W. Helstrom, Minimum mean-squared error of estimates in quantum statistics, *Phys. Lett. A* **25**, 101 (1967).
- [10] K. Matsumoto, A new approach to the Cramér-Rao-type bound of the pure-state model, *J. Phys. A: Math. Gen.* **35**, 3111 (2002).
- [11] R. D. Gill and M. I. Guta, in *On Asymptotic Quantum Statistical Inference* (Institute of Mathematical Statistics, Beachwood, OH, 2013), p. 105.
- [12] L. Pezzè, M. A. Ciampini, N. Spagnolo, P. C. Humphreys, A. Datta, I. A. Walmsley, M. Barbieri, F. Sciarrino, and A. Smerzi, Optimal Measurements for Simultaneous Quantum Estimation of Multiple Phases, *Phys. Rev. Lett.* **119**, 130504 (2017).
- [13] J.-D. Yue, Y.-R. Zhang, and H. Fan, Quantum-enhanced metrology for multiple phase estimation with noise, *Sci. Rep.* **4**, 5933 (2014).
- [14] M. Zuppardo, J. P. Santos, G. De Chiara, M. Paternostro, F. L. Semião, and G. M. Palma, Cavity-aided quantum parameter estimation in a bosonic double-well Josephson junction, *Phys. Rev. A* **91**, 033631 (2015).
- [15] T. J. Proctor, P. A. Knott, and J. A. Dunningham, Multiparameter Estimation in Networked Quantum Sensors, *Phys. Rev. Lett.* **120**, 080501 (2018).
- [16] A. J. den Dekker and A. van den Bos, Resolution: A survey, *J. Opt. Soc. Am. A* **14**, 547 (1997).
- [17] P. R. Hemmer and T. Zapata, The universal scaling laws that determine the achievable resolution in different schemes for super-resolution imaging, *J. Opt.* **14**, 083002 (2012).
- [18] C. Cremer and R. B. Masters, Resolution enhancement techniques in microscopy, *Eur. Phys. J. H* **38**, 281 (2013).
- [19] Lord Rayleigh, Investigations in optics, with special reference to the spectroscope, *Philos. Mag. J. Sci.* **8**, 261 (1879); **8**, 403 (1879); **8**, 477 (1879).
- [20] L. Schermelleh, R. Heintzmann, and H. Leonhardt, A guide to super-resolution fluorescence microscopy, *J. Cell Biol.* **190**, 165 (2010).
- [21] M. Tsang, R. Nair, and X.-M. Lu, Quantum Theory of Superresolution for Two Incoherent Optical Point Sources, *Phys. Rev. X* **6**, 031033 (2016).
- [22] R. Nair and M. Tsang, Far-Field Superresolution of Thermal Electromagnetic Sources at the Quantum Limit, *Phys. Rev. Lett.* **117**, 190801 (2016).
- [23] S. Z. Ang, R. Nair, and M. Tsang, Quantum limit for two-dimensional resolution of two incoherent optical point sources, *Phys. Rev. A* **95**, 063847 (2017).
- [24] C. Lupo and S. Pirandola, Ultimate Precision Bound of Quantum and Subwavelength Imaging, *Phys. Rev. Lett.* **117**, 190802 (2016).
- [25] J. Rehacek, M. Paúr, B. Stoklasa, Z. Hradil, and L. L. Sánchez-Soto, Optimal measurements for resolution beyond the Rayleigh limit, *Opt. Lett.* **42**, 231 (2017).
- [26] R. Kerviche, S. Guha, and A. Ashok, Fundamental limit of resolving two point sources limited by an arbitrary point spread function, in *Proceedings of the IEEE International Symposium on Information Theory (ISIT)* (IEEE, Aachen, 2017), pp. 441–445.
- [27] M. Tsang, Conservative classical and quantum resolution limits for incoherent imaging, *J. Mod. Opt.* **65**, 1385 (2018).
- [28] S. Zhou and L. Jiang, A modern description of Rayleigh's criterion, [arXiv:1801.02917](https://arxiv.org/abs/1801.02917).
- [29] M. Paur, B. Stoklasa, Z. Hradil, L. L. Sanchez-Soto, and J. Rehacek, Achieving the ultimate optical resolution, *Optica* **3**, 1144 (2016).
- [30] F. Yang, A. Taschilina, E. S. Moiseev, C. Simon, and A. I. Lvovsky, Far-field linear optical superresolution via heterodyne detection in a higher-order local oscillator mode, *Optica* **3**, 1148 (2016).
- [31] W. K. Tham, H. Ferretti, and A. M. Steinberg, Beating Rayleigh's Curse by Imaging Using Phase Information, *Phys. Rev. Lett.* **118**, 070801 (2017).
- [32] F. Yang, R. Nair, M. Tsang, C. Simon, and A. I. Lvovsky, Fisher information for far-field linear optical superresolution via homodyne or heterodyne detection in a higher-order local oscillator mode, *Phys. Rev. A* **96**, 063829 (2017).
- [33] A. Chrostowski, R. Demkowicz-Dobrzański, M. Jarzyna, and K. Banaszek, On superresolution imaging as a multiparameter estimation problem, *Int. J. Quantum Inf.* **15**, 1740005 (2017).
- [34] J. Rehacek, Z. Hradil, B. Stoklasa, M. Paúr, J. Grover, A. Krzic, and L. L. Sánchez-Soto, Multiparameter quantum metrology of incoherent point sources: Towards realistic superresolution, *Phys. Rev. A* **96**, 062107 (2017).
- [35] D. Petz and C. Ghinea, Introduction to quantum Fisher information, in *Quantum Probability and Related Topics* (World Scientific, Singapore, 2011), Vol. 27, pp. 261–281.
- [36] J. Suzuki, Explicit formula for the Holevo bound for two-parameter qubit-state estimation problem, *J. Math. Phys.* **57**, 042201 (2016).
- [37] C. Vaneph, T. Tufarelli, and M. G. Genoni, Quantum estimation of a two-phase spin rotation, *Quantum Meas. Quantum Metrol.* **1**, 12 (2013).
- [38] P. J. D. Crowley, A. Datta, M. Barbieri, and I. A. Walmsley, Tradeoff in simultaneous quantum-limited phase and loss estimation in interferometry, *Phys. Rev. A* **89**, 023845 (2014).
- [39] S. Ragy, M. Jarzyna, and R. Demkowicz-Dobrzański, Compatibility in multiparameter quantum metrology, *Phys. Rev. A* **94**, 052108 (2016).
- [40] J. M. Bernardo and A. F. M. Smith, *Bayesian Theory* (Wiley, Sussex, 2000).